TENSION SOFTENING CHARACTERISTICS IMMEDIATELY AFTER CRACKING OF SHORT FIBER REINFORCED MORTAR

K. Yamada[1], T. Homma[1] and S. Ishiyama[1]

[1]Department of Architecture and Environmental Engineering, Akita Prefecture University, Honjo, 015-0055, Japan

ABSTRACT

It is well known that the key material properties to treat cracking in concrete are what described in tension softening diagram (TSD). In the field of fiber reinforced cementitious composite (FRC), it is important to observe the very early stage of cracking which precedes apparent cracking, because it would bear the signs that predict the following cracking and the behavior after cracking. There were few studies discussing the issue related to fiber functioning at early stage of cracking with employing TSD. To investigate the fiber functioning at early stage of cracking, closure stress of plain matrix was subtracted from that of composite applying mixture rule. The same procedure was used to investigate the growth of closure stress that is dependent on the maturity. Although the mere observation of TSDs cannot clearly explicate the fiber functioning, above-mentioned approach revealed some interesting phenomena, otherwise not detected. Increasing or decreasing effect of fiber to tension softening initial stress (Ft) was identified by this method. Polypropylene fiber has a propensity to decrease Ft, whereas alkaline resistant glass fiber (ARG) has an increasing effect. It was unknown so far that the fiber bridging stress of Polypropylene fiber remained constant between 20 and 80micro m in COD regardless of the diameter of fiber and length. The fiber bridging stress of ARG diminishes until COD becomes 80micro m due to fiber breakage when cracking and while mixing. Poly vinyl alcohol fiber has special phenomena between 5 and 30micro m in COD, where fiber bridging stress soared in dried specimen, while it subsided in wet specimen. The former may be derived from rupture of limited numbers of fiber or local catastrophic debonding, and the latter may be from Cook-Gordon effect.

1 INTRODUCTION

The ductile fiber-reinforced cementitious composite (FRC) might owe its development to the bringing fracture mechanics into the field of concrete. One of the most valuable finding in the field of FRC is that the key material properties are tension softening diagram (TSD) and fracture energy (G_F) which can be obtained from TSD.

TSD is a diagram that represents closure stress in the function of crack width. Fig.1 represents typical TSDs: one for plain matrix and the other for FRC. TSD describes essential information of the fiber composites such as tensile strength, energy dissipation due to cracking (G_F) and the maximum crack width when closure stress becomes naught (W_{cr}).

The shapes of TSD for plain cementitious matrix are usually modeled to be a bi-linear function or a curvilinear function similar to it that are comprised of two parts. The first half part of TSD is featured by steep declination, which has been considered to be reflecting micro crack extension in the specimen. The second half part of TSD appears with gradual declining propensity, which has been regarded as the reflection of bridging of aggregate. These basic postulation regarding TSD was discussed by Nomura and Mihashi [1] dividing G_F into the contribution from first half and the latter half of TSD. Mihashi [2, 3] also indicated that the first half of TSD is governed by all the processes from initiation to formation of apparent crack, and it significantly affects the brittleness of matrix.

In the case of fiber composites, the second half of TSD is immediately overwhelmed by fiber bridging effect. Mihashi[4] referred to toughening mechanisms of FRC that consists of zone shielding by small cracks, crack deflection due to aggregates and fiber bridging that mostly affect the performance.

Table 1 Mix proportion

Molding	Matrix	Reinforce	Dry-Wet	Cure	V. F. %	S/C	W/C	W/Powder
Extrusion	RPC	Plain	R. T.	W28	0.0	-	-	0.126
		PP	R. T.	W28	1.0	-	-	0.126
		PVA	R. T.	W28	1.0	-	-	0.126
Extrusion	Cement	Plain	R. T.	AC	0.0	0.88	0.38	0.200
		My	R. T.	AC	1.8	0.88	0.38	0.190
		Tl	R. T.	AC	1.8	0.88	0.38	0.190
		ARG	R. T.	AC	1.8	0.88	0.38	0.190
Cast	Cement	Plain	R. T.	W7	0.0	0.50	0.40	-
		Plain	R. T.	W14	0.0	0.50	0.40	-
		Plain	R. T.	W28	0.0	0.50	0.40	-
	Cement	Plain	Dry	W28	0.0	0.50	0.40	-
		Plain	Wet	W28	0.0	0.50	0.40	-
		PVA	Dry	W28	0.0	0.50	0.40	-
		PVA	Wet	W28	0.0	0.50	0.40	-

Legend
RPC:
Reactive powder composite
V. F.:
Volume fraction of fiber
S/C:
Fraction of Sand/Cement
W/C:
Water to cement ratio
W/Powder:
Fraction of Water/Powder
R.T.:
Dried at room temperature for 18 hours
W7, W14, W28:
Cured in water 7, 14 or 28 days
AC: Autoclaved at 150

Wang and Li [5] measured TSDs of various synthetic-fiber FRCs and observed fractured surface by scanning electron microscope. Li [6] analytically divided closure stress into contribution of fiber bridging stress, aggregate bridging stress, fiber prestress and stress loss by Cook-Gordon effect of steel fiber FRC. This kind of approach, which aims at discussing mechanisms about closure stress development through detailed investigation into TSD, is what authors take in this paper. The authors [7] have been investigating TSD of FRC, and successfully divided closure stress into contribution of matrix and fiber bridging effect. In the same context, this paper focuses on some characteristics in developing closure stress at early stage of cracking.

2 EXPERIMENT

Fourteen types of mixtures made of three types of matrix that were reinforced with five different types of short fibers were used for experiment, which are listed in Table 1. Table2 refers to fiber reinforcement in Table 1.

Bending test was executed employing plate specimens measured 13.5mm in height and 38.5mm in width. In the bending test, load was applied at center of span that was 150mm, and load and deflection at center was measured. Fracture mechanics test was also executed utilizing prism

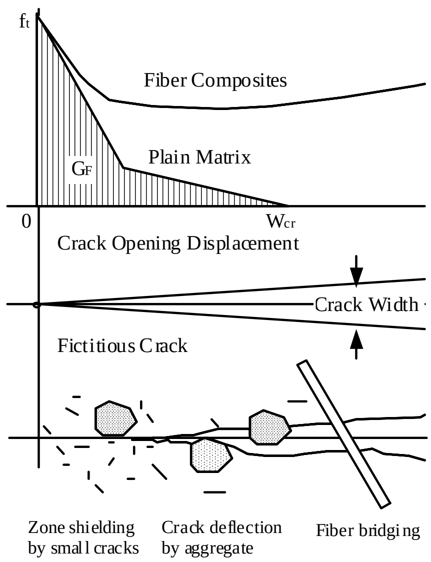

Figure 1 Modeled crack and TSD

Table 2 Mechanical Properties of Short Fiber in Table 1

Type	Name	Diameter mm	Length mm	Modulus GPa	Strength GPa
Polypro-pylene	PP	0.110	12.0	10.0	0.410
	My	0.018	6.0	6.4	0.250
	Tl	0.040 x 0.215	6.0	12.0	0.490
Alkaline resistant glass	ARG	0.018 (Mono-filament)	6.0	74.0	1.400
Polyvinyl Alcohol	PVA	0.100	12.0	31.0	1.100

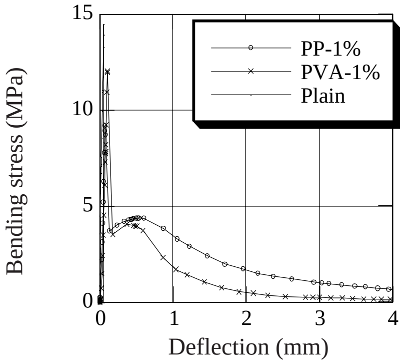

Figure 2 Bending diagram of RPC matrix

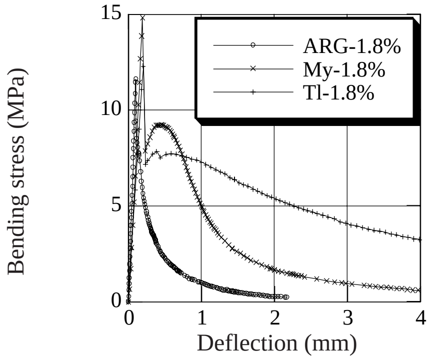

Figure 3 Bending diagram of AC matrix

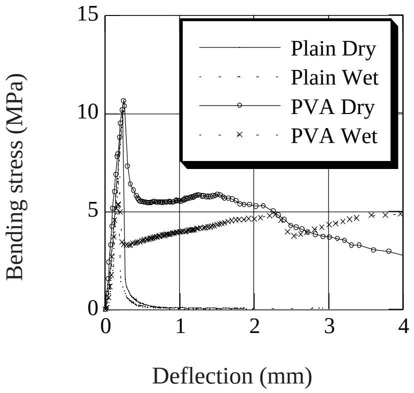

Figure 4 Bending diagram of cast cement matrix

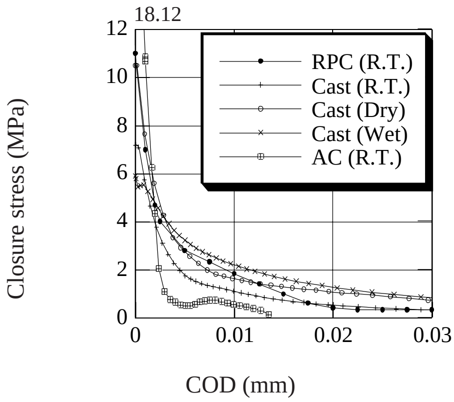

Figure 5 TSD for 5 types of plain matrix

specimens measured 38.5mm in height and width, which has a half-depth notch at center. In the fracture mechanics test, load was applied at center of span that was 150mm, and load and crack opening displacement (COD) was measured at very low speed (0.002mm/s). The result of it was analyzed with employing poly-linear approximation reverse analysis [8, 9], and finally TSD was obtained.

2 RESULTS

Figure 2 to 4 represents all of the bending behaviors. After primary cracking, characteristic bending behaviors were observed. Figure 5 represents all of the TSDs of plain matrices. The highest tension softening initial stress (Ft) appeared in Autoclave cured cement matrix (18.12MPa) The second highest stress appeared in RPC cured in water for 28days, which is naturally lower than that of ordinary RPC cured in steam at 90℃. Others were cast cement matrix cured in water for 28days, which has different water content ratios: R.T. has 12% (room dried), Dry has 0% and Wet has 18% (saturated) of it. Because Dry suffers 100℃ for 48 hours which progress the hydration, Ft is higher than that of others. The AC specimen was composed of only powdery materials (powdered silica and cement) which measure about 15 to 20micro m in average diameter closure stress decays at about 15micro m. The COD which keeps closure stress is about 60 to 80micro m for others, because they contain sand aggregate under 2.36mm in sift size.

Figure 6 represents the growth of TSD of plain matrix. It is observed that the growth of closure stress

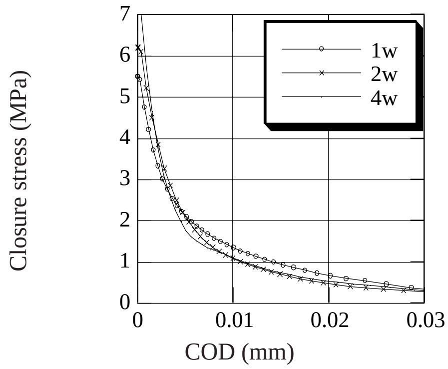

Figure 6 TSD for W7, W14 and W28 matrix

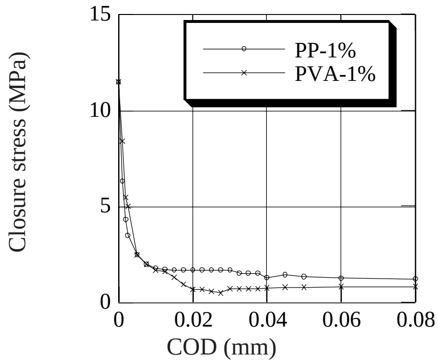

Figure 7 TSD for RPC matrix

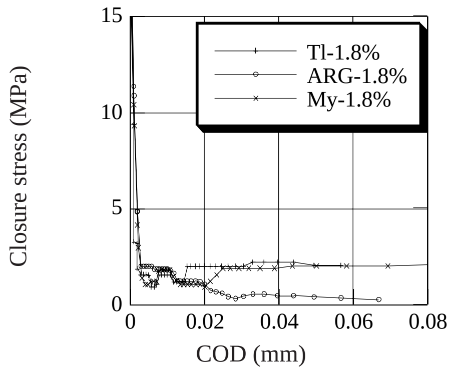

Figure 8 TSD for AC matrix

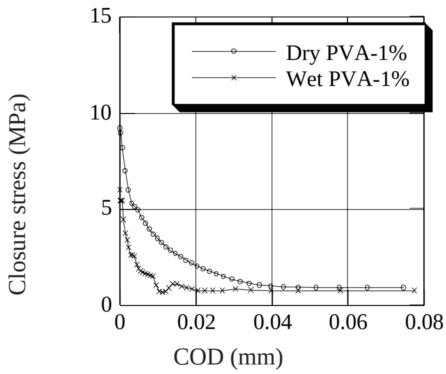

Figure 9 TSD for W28 matrix

mostly appears in Ft. Figure 7 to 9 represent TSDs in the cases of fiber-reinforced matrices. Except for the case of ARG, closure stress was about 1.5MPa per 1% of fiber reinforcement when COD is 0.08mm. All of the TSDs were different but the difference cannot distinctly be described in this type of plot.

3 DISCUSSION

Closure stress can be divided into contributions of fiber and matrix with employing mixture rule [10] as described in following eqn (1).
In it, σ (t) is closure stress of composites, η is fiber coefficient, V_f and V_m are volume fraction of fiber and matrix, and σ (f) and σ (m) are closure stress of fiber and matrix. Therefore, the first term of eqn (1), which is the contribution of fiber, can be extracted by subtracting closure stress of plain matrix from that of composite. Following the same procedure, the growth of closure stress of plain matrix according to the curing duration (maturity) can be extracted by eqn (2). In it, σ_b is closure stress at maturity b, σ_a is closure stress at maturity a, and $\Delta\sigma_{a-b}$ is increase of closure stress during a and b.

$$\sigma(t) = \eta V_f \sigma(f) + V_m \sigma(m) \quad (1)$$
$$\sigma_b = \sigma_a + \Delta\sigma_{a-b} \quad (2)$$

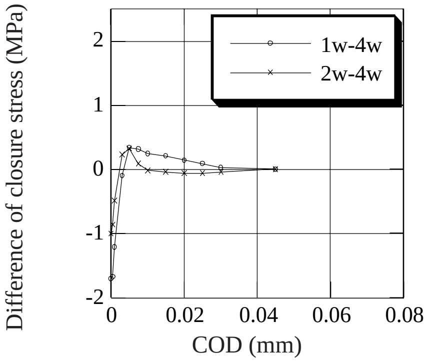

Figure 10 Growth of closure stress

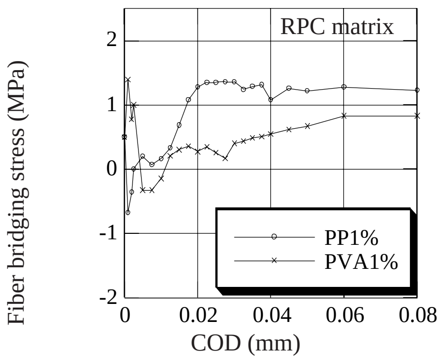

Figure 11 Fiber bridging stress for RPC matrix

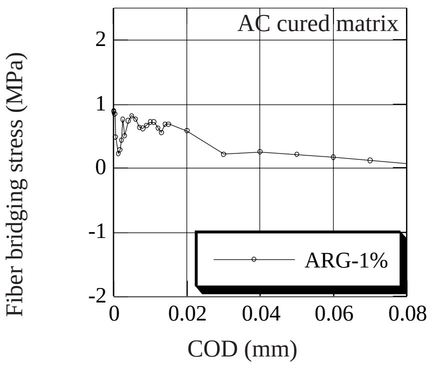

Figure 12 Fiber bridging stress for ARG

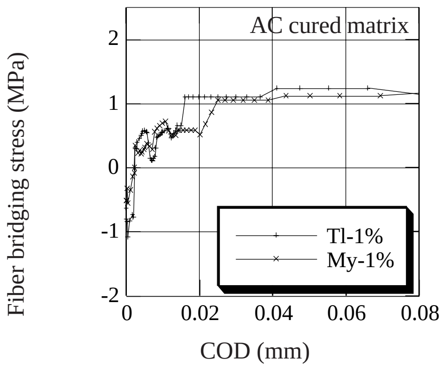

Figure 13 Fiber bridging stress for AC matrix

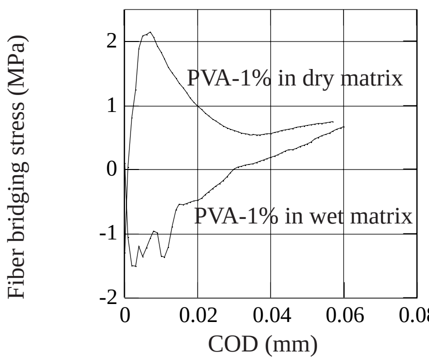

Figure 14 Water content and fiber bridging stress

Figure 10 represents the development of closure stress which corresponds to Figure 6. That means $\Delta\sigma_{a-b}$ where a is 1 week or 2 weeks, and b is 4 weeks in eqn (2). It is obvious that the increase of Ft is obtained in exchange for the loss of closure stress between 10 to 20micro m.

Figure 11 to 14 represent fiber bridging stress obtained by eqn (1), whose TSDs correspond to Figure 7 to 9. In the case that fiber volume fraction was 1.8%, the obtained stress was divided by 1.8 to set equal the fraction (1%). From these, it can be said that polypropylene fibers (PP, Tl and My) tend to have negative values near crack initiation, which implies the notch effect of decreasing Ft. On the contrary, Figure 12 shows that ARG has positive value at initial cracking, which means the increase of Ft. The closure stress of polypropylene fibers has constant value (1.1MPa: AC, 1.3MPa: RPC) up to 80micro m, whereas that of ARG immediately decreases. The reason of this difference of fiber effect derives from the properties of fiber: elastic modulus, affinity to matrix and the effective fiber length in specimen because ARG easily breaks during mixing. It looks strange that the closure stress does not depend on the matrix and fiber diameter, which suggest the total fiber volume governs the bridging stress in this very early stage of cracking.

The interesting finding is that the water content ratio has significant effect on fiber bridging for PVA, which can be observed from Figure 14. In the case of dry condition, the increase of fiber bridging stress may be ascribed to following possibilities: the rupture of limited numbers of fiber due to decreased tensile strength by drying process, or local catastrophic debonding of limited numbers of fiber due to enhanced cohesive strength by drying process. In the case of wet condition, some negative effect occurred in closure stress between 5 and 15micro m in COD. This phenomenon may be the result of Cook-Gordon effect [11] due to the weakened cohesive strength by water layer around fiber.
It should be paid attention to that the crack width is the nominal value based on fictitious model [12], but there are some significant phenomena appear in the early stage of cracking as discussed above.

4 CONCLUSIONS

To investigate the effect of fiber in early stage of cracking, closure stress of plain matrix was subtracted from that of composite applying mixture rule. The same procedure was used to investigate growth of closure stress according with the maturity. Although the mere observation of TSDs cannot clearly explicate the functioning of the fiber, above-mentioned approach revealed some interesting phenomena, otherwise not detected.
(1) Increasing or decreasing effect of fiber to tension softening initial stress was identified.
(2) Some special phenomena at early stage of cracking were successfully detected.

REFERENCES

[1] Nomura, N., Mihashi, H. and Izumi, M.: Tension Softening Behavior and Mechanism of Fracture Energy Absorption in Concrete, J. of Str. & Constr. Engng., AIJ, No. 438, Aug. 1992, pp.9-14.
[2] Mihashi, H., Nomura, N. and Kirikoshi, K.: Mechanical Properties of FRCC on the Basis of Fracture Mechanics, J. of Str. & Constr. Engng., AIJ, No. 449, 1993, pp.1-7.
[3] Mihashi, H.: Influence of Strength Properties of Concrete on Fracture Mechanics Parameters, Concrete Research and Technology, Vol. 6, No. 1, Jan. 1995, pp.81-88.
[4] Mihashi, H.: Application of Fracture Mechanics into Material Design of Cementitious Composites, Proceedings of the JCI, Vol.12, No. 1, 1990, pp.1175-1180.
[5] Wang, Y., Li, V. C. and Backer, S.: Tensile Failure Mechanisms in Synthetic Fiber-reinforced Mortar, J. of Materials Science, No. 26, 1991, pp.6565-6575.
[6] Li, V. C., Stang, H. and Krenchel, H.: Micromechanics of cracked bridging in fiber-reinforced concrete, Materials and structures, No. 26, 1993, pp.486-494.
[7] Yamada, K., Ishiyama, S. and Homma, T.: Tension Softening Approach to Enhancement of Ductility of Extruded Cement Composites, Proc. of the JCI Workshop on DFRCC, JCI, Oct. 2002, pp.103-112.
[8] Kitsutaka, Y., Uemura, K., Nakamura, S.: Reverse analysis to achieve tension softening curve of concrete as approximated polylinear relation, J. of Str. & Constr. Engng., No. 453, 1993, pp.15-25.
[9] Rokugo K., Uchida Y., Kurihara N., Koyanagi, W.: Determination of Tension Softening Diagram of Concrete through Poly-linear Approximation Analysis and Application to Fiber Reinforced Concrete, Advances in Building Materials Science, AEDIFICATIO, 1996, pp.43-58.
[10] Hannant, D. J.: Fiber cements and fiber concretes, John Wiley & Sons, 1978, 219pages.
[11] Bentur, A., and Mindess, S.: Fiber Reinforced Cementitious Composites, Elsevier Applied Science, 1990, 449pages.
[12] Hillerborg, A.: The Theoretical Basis of a Method to Determine the Fracture Energy G_F of Concrete, Materials and Structures, RILEM, Vol. 18, No. 106, 1985, pp.25-30.